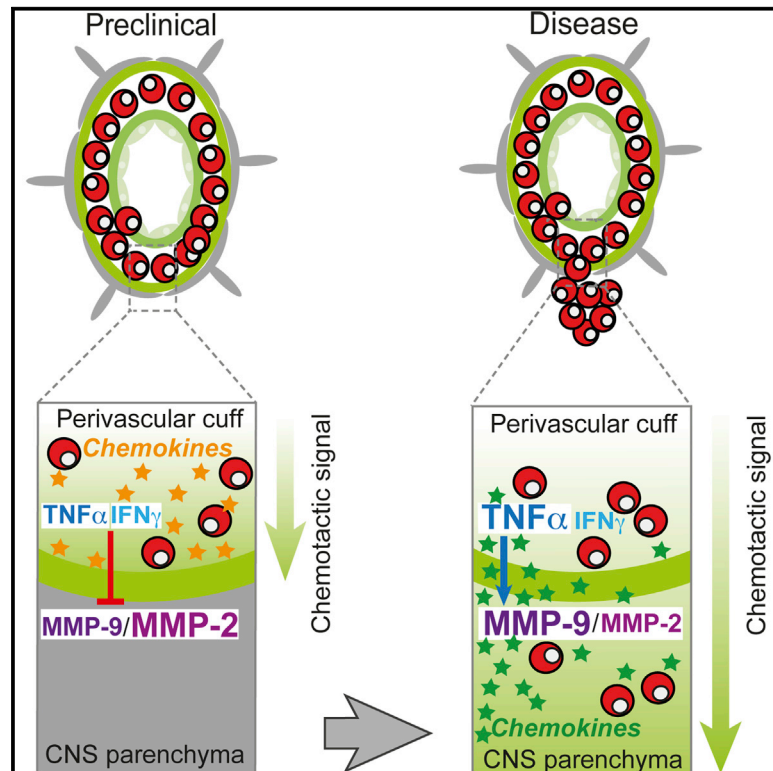# Focal MMP-2 and MMP-9 Activity at the Blood-Brain Barrier Promotes Chemokine-Induced Leukocyte Migration

Graphical Abstract

Authors

Jian Song, Chuan Wu, ...,
Rupert Hallmann, Lydia Sorokin

Correspondence

sorokin@uni-muenster.de

In Brief

Chemokines are required for leukocyte migration into the CNS; however, additional MMP-2/9 activity specifically at the border of the CNS parenchyma strongly enhances this transmigration process. Song et al. show that cytokines derived from infiltrating leukocytes regulate MMP-2/9 activity at the parenchymal border, which differentially modulates chemokine activities, thereby accelerating leukocyte migration into the CNS.

Highlights

- MMP-2 and MMP-9 activity occurs at the blood-brain barrier

- Cytokines derived from infiltrating leukocytes control MMP activity at the BBB

- MMPs modulate chemokines at the BBB required for leukocyte chemotaxis

- Cytokines, chemokines, and MMPs act together to accelerate leukocyte chemotaxis

Focal MMP-2 and MMP-9 Activity at the Blood-Brain Barrier Promotes Chemokine-Induced Leukocyte Migration

Jian Song,[1,4,7] Chuan Wu,[1,7,10] Eva Korpos,[1,4] Xueli Zhang,[1,4] Smriti M. Agrawal,[1,9] Ying Wang,[1] Cornelius Faber,[2,4] Michael Schäfers,[3,4] Heinrich Körner,[5] Ghislain Opdenakker,[6] Rupert Hallmann,[1,4,8] and Lydia Sorokin[1,4,8,*]

[1]Institute of Physiological Chemistry and Pathobiochemistry, University of Muenster, 48149 Muenster, Germany
[2]Department of Clinical Radiology, University of Muenster, 48149 Muenster, Germany
[3]European Institute for Molecular Imaging, University of Muenster, 48149 Muenster, Germany
[4]Cells-in-Motion Cluster of Excellence, University of Muenster, 48149 Muenster, Germany
[5]Menzies Institute for Medical Research, Hobart, TAS 7000, Australia
[6]Department of Microbiology and Immunobiology, Rega Institute for Medical Research, University of Leuven, 3000 Leuven, Belgium
[7]Co-first author
[8]Co-senior author
[9]Present address: University of Calgary, AB T2N 1N4 Calgary, Canada
[10]Present address: Evergrande Center for Immunological Diseases, Hospital Harvard Medical School, Boston, MA 02115, USA
*Correspondence: sorokin@uni-muenster.de
http://dx.doi.org/10.1016/j.celrep.2015.01.037

SUMMARY

Although chemokines are sufficient for chemotaxis of various cells, increasing evidence exists for their fine-tuning by selective proteolytic processing. Using a model of immune cell chemotaxis into the CNS (experimental autoimmune encephalomyelitis [EAE]) that permits precise localization of immigrating leukocytes at the blood-brain barrier, we show that, whereas chemokines are required for leukocyte migration into the CNS, additional MMP-2/9 activities specifically at the border of the CNS parenchyma strongly enhance this transmigration process. Cytokines derived from infiltrating leukocytes regulate MMP-2/9 activity at the parenchymal border, which in turn promotes astrocyte secretion of chemokines and differentially modulates the activity of different chemokines at the CNS border, thereby promoting leukocyte migration out of the cuff. Hence, cytokines, chemokines, and cytokine-induced MMP-2/9 activity specifically at the inflammatory border collectively act to accelerate leukocyte chemotaxis across the parenchymal border.

INTRODUCTION

Chemokines are central for migration of several cell types; however, their levels and efficacy of action depend on additional factors, such as cytokines and/or their selective proteolytic processing. Particularly in models of autoimmunity, T cell-derived cytokines define the characteristics of different T cell subpopulations and play decisive roles in shaping the microenvironment within the target organ, which collectively regulate immune cell infiltration. Experimental autoimmune encephalomyelitis (EAE) is a widely used T cell-mediated model for the early inflammatory stages of multiple sclerosis (MS) that depends on a special microenvironment at the blood-brain barrier (BBB). Due to a unique double-basement membrane structure of cerebral blood vessels (Sixt et al., 2001), EAE has proven to be a valuable model for investigating the steps in leukocyte migration into the CNS. Initial penetration of the BBB requires transmigration of the endothelial monolayer and its underlying endothelial basement membrane, followed by accumulation in the perivascular space where leukocytes are retained for several days. Within the perivascular cuff, leukocytes are reactivated and the balance of effector versus regulatory T cell populations is determined (Körner et al., 1997), which permits subsequent transmigration of the parenchymal basement membrane and glia limitans and infiltration of the CNS parenchyma. Only then do disease symptoms become apparent, indicating that migration out of the perivascular cuff is a disease-limiting step (Agrawal et al., 2006).

Effector T cell populations critical for the pathogenesis of EAE include T helper type 1 (T_H1) and interleukin-17 (IL-17)-producing T helper (T_H17) cells, which differ in their cytokine profiles and, thereby, proinflammatory properties. T_H1 cells are characterized by secretion of tumor necrosis factor (TNF-α) and interferon-γ (IFN-γ), whereas TNF-α and IL-17 are representative of the T_H17 cell lineage (Weaver et al., 2007), which is considered to be a pro-encephalitogenic population. However, precisely how these cytokines influence the different steps in immune cell penetration of tissues remains inconclusive.

Data suggest that penetration of the endothelial and parenchymal barriers are independent steps involving distinct molecular mechanisms. While several factors have been identified that play important roles in penetration of the endothelial cell monolayer (Engelhardt, 2006) and its basement membrane (Sixt et al., 2001; Wu et al., 2009), comparatively little is known about the

subsequent penetration of the parenchymal border. Chemokines such as CXCL12 have been shown to be required for holding T cells in the perivascular cuff, and its proteolytic degradation by MMPs releases leukocytes to migrate into the CNS parenchyma (McCandless et al., 2006). TNF-α also has been implicated in this step as TNF-α knockout ($Tnf^{-/-}$) mice show massively enlarged perivascular cuffs and delayed onset of disease symptoms (Körner et al., 1997). Although the precise mechanism of TNF-α action is not clear, differences in chemokine profiles in the CNS of $Tnf^{-/-}$ mice compared to wild-type (WT) littermates have been proposed to delay the initial leukocyte penetration of the parenchymal barrier (Murphy et al., 2002). In addition, in situ zymography has revealed matrix metalloproteinase (MMP)-2 and MMP-9 activity at sites of leukocyte penetration of the parenchymal border (Agrawal et al., 2006). Young MMP-9 knockout mice are partially resistant to EAE (Dubois et al., 1999), while MMP-2 and MMP-9 double-knockout (DKO) mice are completely resistant to disease development (Agrawal et al., 2006), suggesting a central role for these MMPs in disease induction.

In addition to CXCL12, several chemokines play a role in leukocyte recruitment in EAE (Ransohoff, 2009), some of which are constitutively expressed in the CNS parenchyma and upregulated during EAE and others that are newly synthesized (Ambrosini et al., 2005; Glabinski et al., 1995; Murphy et al., 2002). However, CNS-specific chemokine expression never precedes histopathological signs of EAE (Glabinski et al., 1995; Huang et al., 2000), indicating that initial leukocyte infiltration into the CNS is a prerequisite for the expression of chemokines. Proinflammatory cytokines secreted from infiltrating cells, including TNF-α, IFN-γ, and IL-17, can directly influence chemokine levels by inducing mRNA expression (Murphy et al., 2002) and stability (Hartupee et al., 2007), but they also can have indirect effects by modulating protease levels and activities, including those of MMPs, which in turn can alter chemokine activation or inactivation and their expression (Corry et al., 2002; McQuibban et al., 2000; Van den Steen et al., 2000).

Using bone marrow (BM) chimeric mice lacking immune-cell or tissue-resident sources of MMP-2 and MMP-9 or TNF-α in EAE experiments combined with in vitro studies, we show here that inflammatory cytokines, chemokines, and activated MMP-2 and MMP-9 act in concert at the parenchymal border to determine whether or not leukocyte infiltration into the CNS parenchyma occurs.

RESULTS

Mice Lacking MMP-2 and MMP-9 in Immune and Tissue-Resident Cells Have Enlarged Perivascular Cuffs

To distinguish between infiltrating leukocyte and CNS-resident sources of the gelatinases, WT, $Mmp2^{-/-}$ or $Mmp9^{-/-}$, and DKO recipients carrying WT BM, and therefore WT leukocytes, were actively induced for EAE. Conversely, DKO BM was transferred to WT recipients to generate mice lacking a leukocyte source of MMP-2/9, and EAE was actively induced. In the absence of a tissue-resident or leukocyte source of MMP-2 and MMP-9, the appearance of EAE symptoms was delayed and disease symptoms were less severe than in WT or single-

KO chimeric mice (Figure 1A), indicating that MMP-2/9 from both leukocytes and resident cells contribute to EAE induction and severity.

No differences were measured in numbers of CD45$^+$ leukocytes, CD4$^+$ or CD8$^+$ T cells, and CD11b$^+$ macrophages in the CNS during EAE in any of the chimeric mice carrying WT BM. Only WT mice carrying DKO BM showed lower numbers of all immune cells (Figures 1B, 1C, S1A, and S1B), suggesting an impaired immune response in the absence of leukocyte-derived MMP-2 and MMP-9. Since these chimeric mice develop EAE symptoms, T cell priming in the periphery may be less efficient than when MMPs are expressed by immune cells but activated effector T cells can be generated. This was confirmed by in vitro experiments that revealed a reduced antigen-specific response of DKO CD4$^+$ T cells (Figure S1C), but an absence of defects in anti-CD3-induced T cell proliferation (Figure S1D).

Immunofluorescence staining of brain and spinal cord sections, using antibodies to pan-laminin and CD45 to visualize the endothelial and parenchymal basement membranes and infiltrating leukocytes, suggested enlarged perivascular cuffs in mice lacking an immune-cell or tissue-resident source of MMP-2 and MMP-9 (Figure 1D). Stereological analyses, involving MRI determination of tissue volumes (Figure S1E) and subsequent calculation of cuff numbers and cuff area/brain or spinal cord using serial sections throughout the entire tissue stained for pan-laminin and CD45, revealed that mice lacking a leukocyte or tissue-resident source of MMP-2 and MMP-9 had fewer but larger cuffs at EAE onset (Figures 1E and 1F). At peak EAE, when significant numbers of leukocytes had penetrated the parenchymal border, there were fewer cuffs but they remained enlarged in DKO mice carrying WT BM (Figures S1F and S1G), suggesting a more prominent role of CNS-derived MMPs for penetration of the parenchymal border.

Enlarged cuffs without differences in total immune cell infiltration suggests either enhanced leukocyte migration into or reduced migration out of the cuff. Transfer of CD45.1$^+$ WT MOG$_{35-55}$-specific T cells to CD45.2$^+$ WT, $Mmp2^{-/-}$, $Mmp9^{-/-}$, or DKO recipients and quantification of CD45.1$^+$ T cells in the CNS of recipient mice at day 3 after transfer, before proliferation had commenced (Wu et al., 2009), revealed equal numbers of donor T cells in all recipients (Figures S2A and S2B). This suggests that the enlarged cuffs in mice lacking a resident source of MMP-2 and MMP-9 was due to reduced migration out of the cuff.

In both brains and spinal cords of mice lacking a leukocyte or tissue-resident source of MMP-2 and MMP-9, fewer cuffs showed leukocyte penetration at EAE onset compared to peak (Figure S3A). Immunohistochemistry for myelin basic protein revealed no demyelination (Figure S3B) nor detectable MMP-2/9 activity by in situ zymography surrounding cuffs until leukocyte penetration had occurred and EAE symptoms were apparent (Figures 1D and S3C; Agrawal et al., 2006).

Mice Lacking T Cell-Derived TNF-α Also Have Enlarged Cuffs

Enlarged perivascular cuffs also have been reported in $Tnf^{-/-}$ mice induced for EAE (Körner et al., 1997). As T cell-derived TNF-α has been shown to be responsible for this phenotype
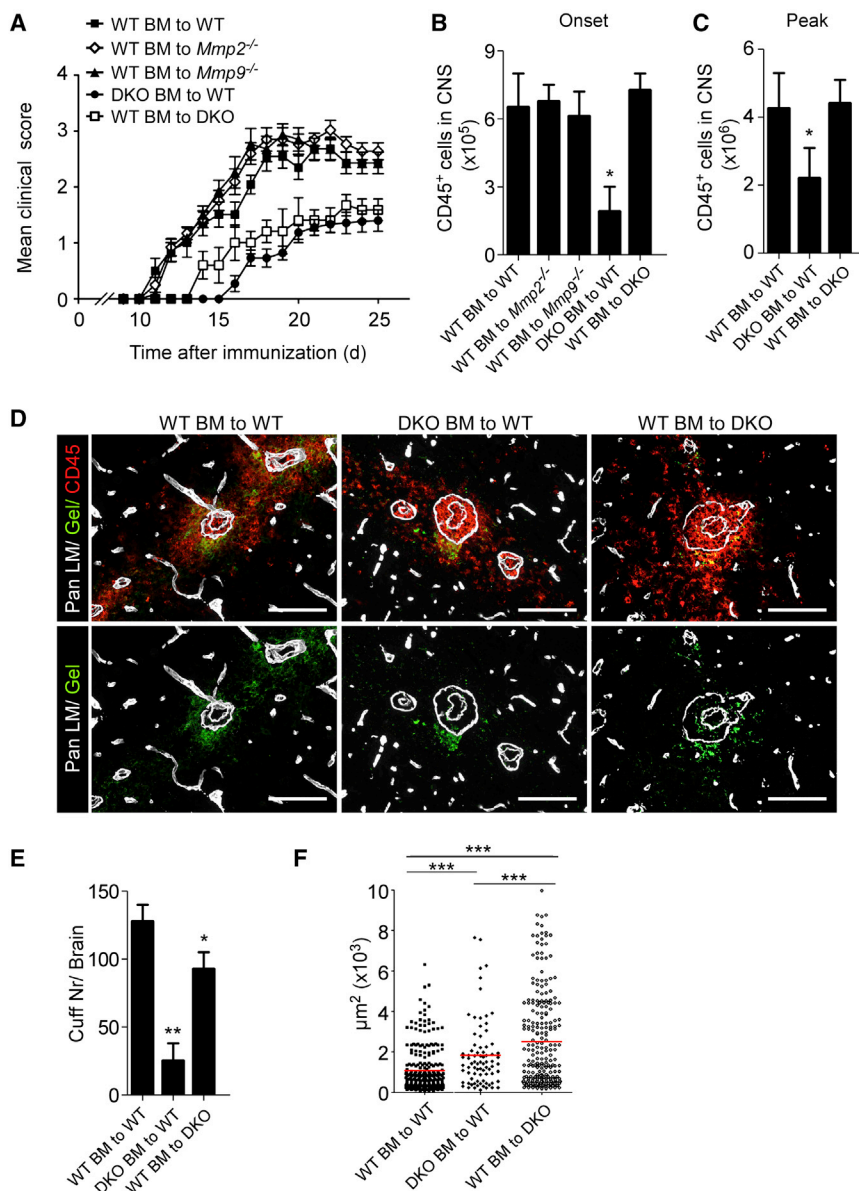
Figure 1. Leukocyte and Tissue-Resident Sources of MMP-2 and MMP-9 Are Required for EAE

(A) Time course of EAE in WT, $Mmp2^{-/-}$, $Mmp9^{-/-}$, and MMP-2 and MMP-9 DKO mice, carrying WT BM, and WT mice carrying DKO BM.

(B and C) Flow cytometry quantification of total donor CD45$^+$ cells in the CNS at onset (days 12–15) and peak EAE (day 20). Data in (A–C) are means ± SEM; each point n = 12.

(D) CNS sections from WT mice carrying WT or DKO BM and DKO mice carrying WT BM at day 17 EAE immunofluorescently stained for CD45$^+$ leukocytes and pan-laminin, to define endothelial and parenchymal basement membranes, and corresponding gelatin in situ zymography for MMP-2 and MMP-9 activity (Gel).

(E and F) Stereological analyses at EAE onset for (E) cuff numbers and (F) sizes. Cuff numbers are means ± SEM of four experiments, with three mice/group; cuff areas are all values measured. Scale bars represent 80 μm. *p < 0.05,**p < 0.01, ***p < 0.001. See also Figures S1–S3.

T Cell-Derived TNF-α/IFN-γ Ratios Control MMP-9 Expression at the BBB

To investigate whether a causal relationship exists between TNF-α and MMP-2/MMP-9 activity at the BBB, we examined cytokine levels in the CNS and the source of MMPs at the parenchymal border. After EAE induction, $Tnf^{-/-}$ mice showed significantly increased proportions of CD4$^+$IFN-γ$^+$ cells in the CNS (Figure 2E), draining lymph nodes (LNs) and spleens (Figure S4I) compared to WT mice. Elevated levels of IFN-γ was corroborated by ELISA of CNS extracts of WT and $Tnf^{-/-}$ mice (Figure 2F). Accordingly, conditioned media from cultured MOG$_{35–55}$-specific $Tnf^{-/-}$ and WT CD4$^+$ T cells contained identical levels of IL-4, IL-10, IL-6, IL-17, and IL-1α, but elevated IFN-γ in $Tnf^{-/-}$ samples (Figure S4J). Hence, $Tnf^{-/-}$ CD4$^+$ T cells not only lack TNF-α, but also have elevated IFN-γ levels throughout the disease course (Figure S4K).

Previous studies have identified MMP-9 secretion by T cells (Dubois et al., 1999) and MMP-2 and MMP-9 by macrophages (Agrawal et al., 2006). In situ hybridization of WT mice carrying DKO BM, and hence no immune-cell source of MMP, showed that astrocytes at the BBB also can express MMP-9, but only after EAE induction (Figure 3A). This was confirmed using qPCR, gel zymography, and ELISA of cultured astrocytes, revealing constitutive expression of pro- and activated MMP-2 and upregulation of pro- and activated MMP-9 by TNF-α and, to a lesser extent, by IL-17 and inhibition by IFN-γ (Figures 3B–3D). A similar trend but with milder effects was observed for MMP-2 (Figures 3B–3D). These results are consistent with the reported effects

(Murphy et al., 2002), we adoptively transferred encephalitogenic $Tnf^{-/-}$ T cells to WT recipients and examined cuff sizes in correlation with MMP-2/9 activity. EAE was delayed and reduced in severity in mice lacking T cell-derived TNF-α (Figure 2A), as observed in $Tnf^{-/-}$ mice induced for EAE (Figure S4A; Körner et al., 1997). Immunofluoresence staining and stereological analyses revealed similarly enlarged cuffs in TNF-α-deficient mice (Figures 2B–2D and S4B–S4F), as observed in the MMP-2/9 BM chimeric mice, with equivalent numbers of immune cells at onset and peak EAE (Figures S4G and S4H), which correlated with no detectable MMP-2 and MMP-9 activity using gel zymography and in situ zymography (Figure 2B). At peak EAE, when considerable numbers of leukocytes had penetrated the parenchymal border, MMP-2/9 activity was detectable and cuff sizes were reduced (Figures 2B–2D and S4B–S4F).
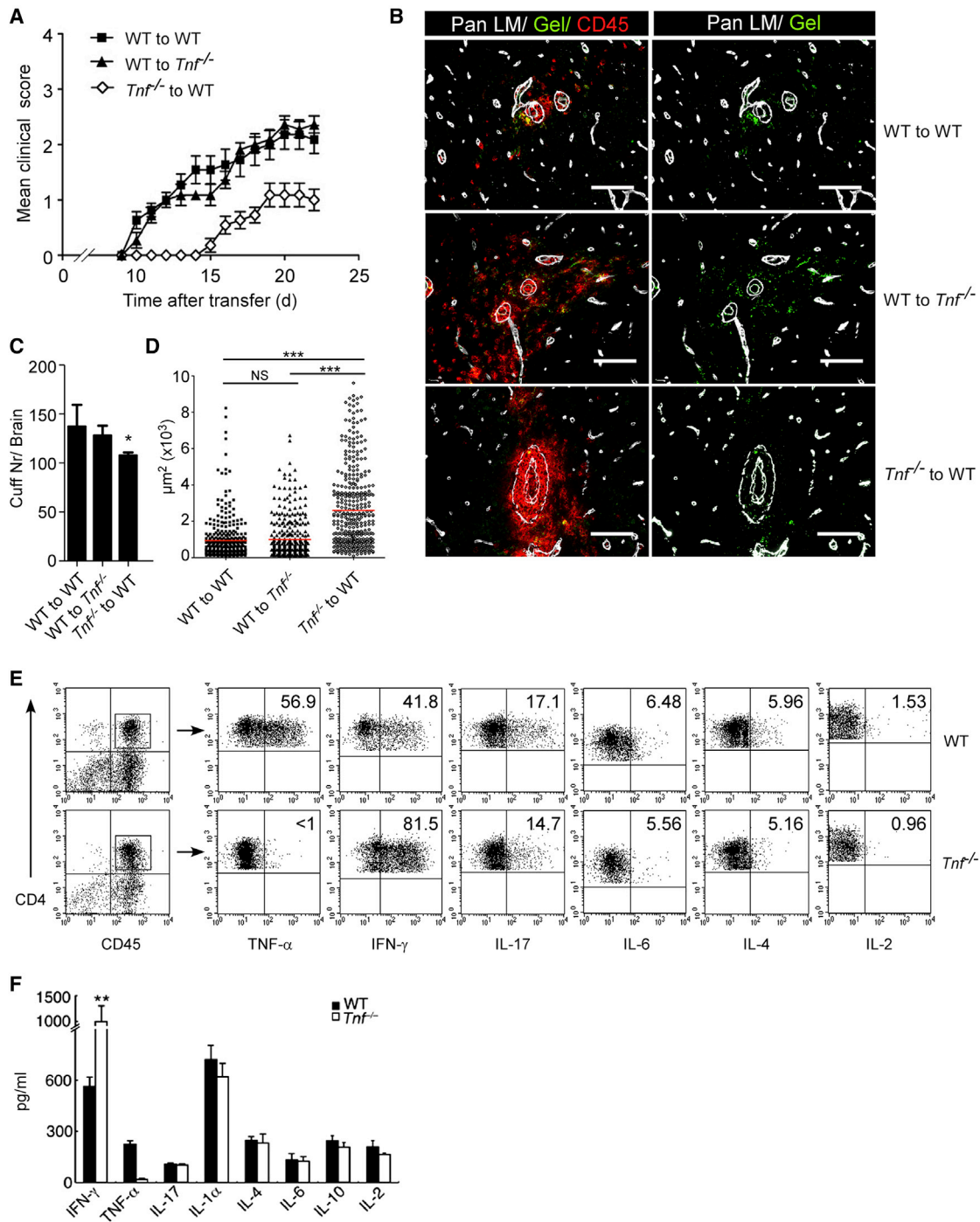
Figure 2. T Cell-Derived Cytokines Regulate Leukocyte Penetration of the Parenchymal Border

(A) Time course of EAE after passive transfer of WT encephalitogenic T cells to WT and $Tnf^{-/-}$ recipients, or $Tnf^{-/-}$ encephalitogenic T cells to WT recipients. Data are means ± SEM from three experiments with six mice/group.

(B) Immunofluorescence staining of day 17 EAE CNS sections for pan-laminin and CD45 and corresponding gelatin in situ zymography for MMP-2 and MMP-9 activity (Gel). Scale bars represent 80 μm.

(C and D) Stereological analyses at EAE onset for (C) cuff numbers and (D) sizes, showing enlarged cuffs in mice lacking a T cell source of TNF-α. Cuff numbers are means ± SEM of three experiments, with three mice/group; cuff areas are all values measured.*p < 0.05, ***p < 0.001.

(E and F) (E) Flow cytometry for intracellular cytokine staining in CD4⁺ T cells from CNS of WT and $Tnf^{-/-}$ mice at day 20 after EAE induction and (F) corresponding total cytokine levels in CNS extracts measured by ELISA. Data are means ± SEM from three experiments, with triplicates/experiment. Values are means of three to four experiments with triplicates/time point or treatment ± SEM. **p < 0.01. See also Figures S4 and S5.
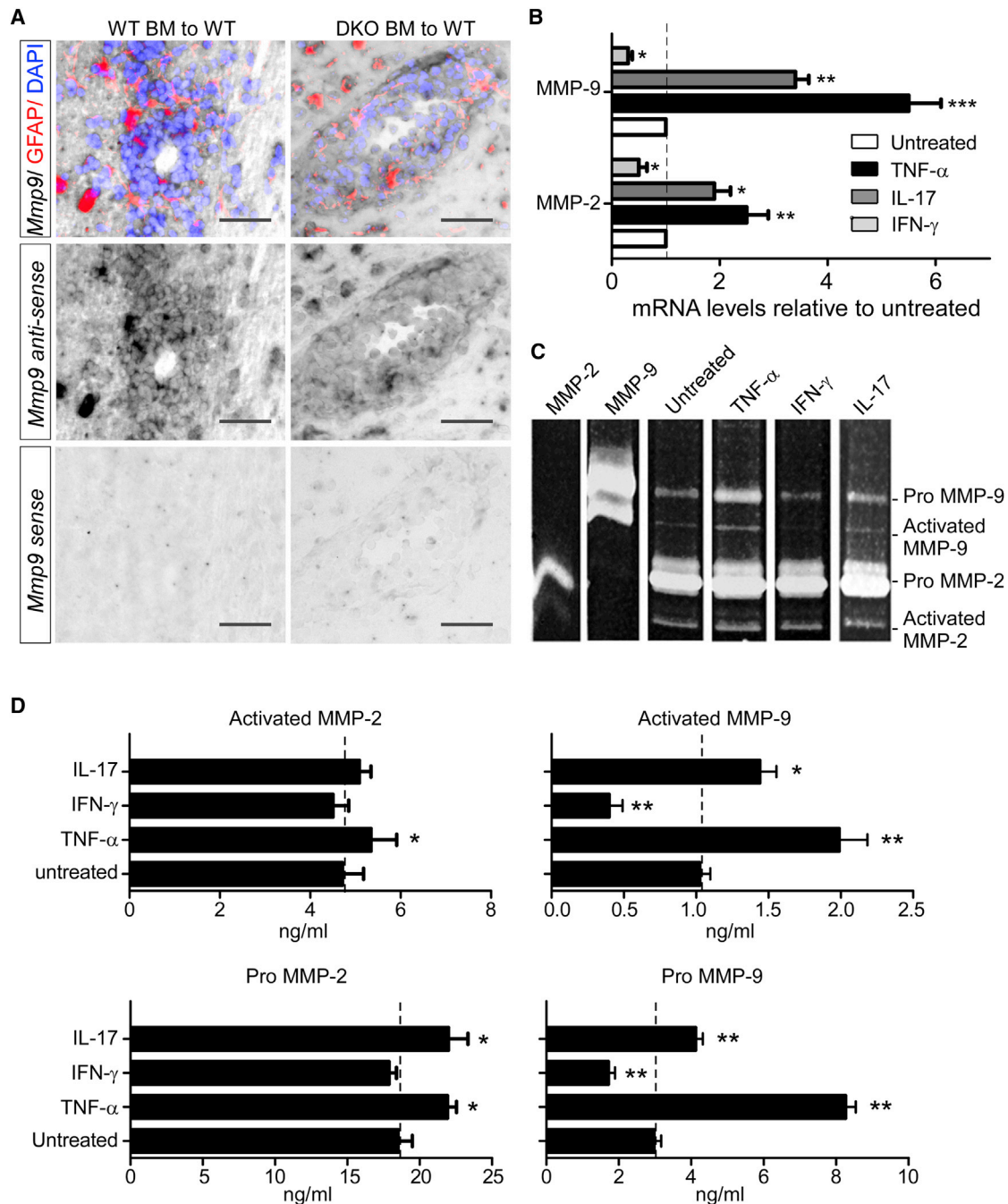
Figure 3. T Cell-Derived Inflammatory Cytokines Regulate Astrocyte Expression of MMP-2 and MMP-9
(A) In situ hybridization of MMP-9 cDNA on brain sections from WT mice carrying WT or DKO BM at days 15–17 of EAE counter-stained for the astrocyte marker GFAP (red) and for DAPI (blue) to show immune cell accumulations.
(B–D) (B) qPCR shows MMP-2 and MMP-9 mRNA expression by WT astrocytes, which is enhanced by TNF-α and IL-17 and reduced by IFN-γ, and is confirmed at the protein level by (C) gelatin gel zymography and (D) ELISA of concentrated, pre-purified conditioned media samples. Scale bar represents 30 μm. *p < 0.05, **p < 0.01, ***p < 0.001.

of cytokines on MMP-2 and MMP-9 expression in other tissues (Rosenberg, 2002). Taken together, the data suggest that MMP-9 secretion by astrocytes at the BBB is enhanced by T cell-derived TNF-α/IL-17 and inhibited by IFN-γ.

MMPs Are Required for Leukocyte Chemotaxis out of the Cuff
As chemokines are required for attracting T lymphocytes into the CNS parenchyma during EAE, we tested the chemotactic
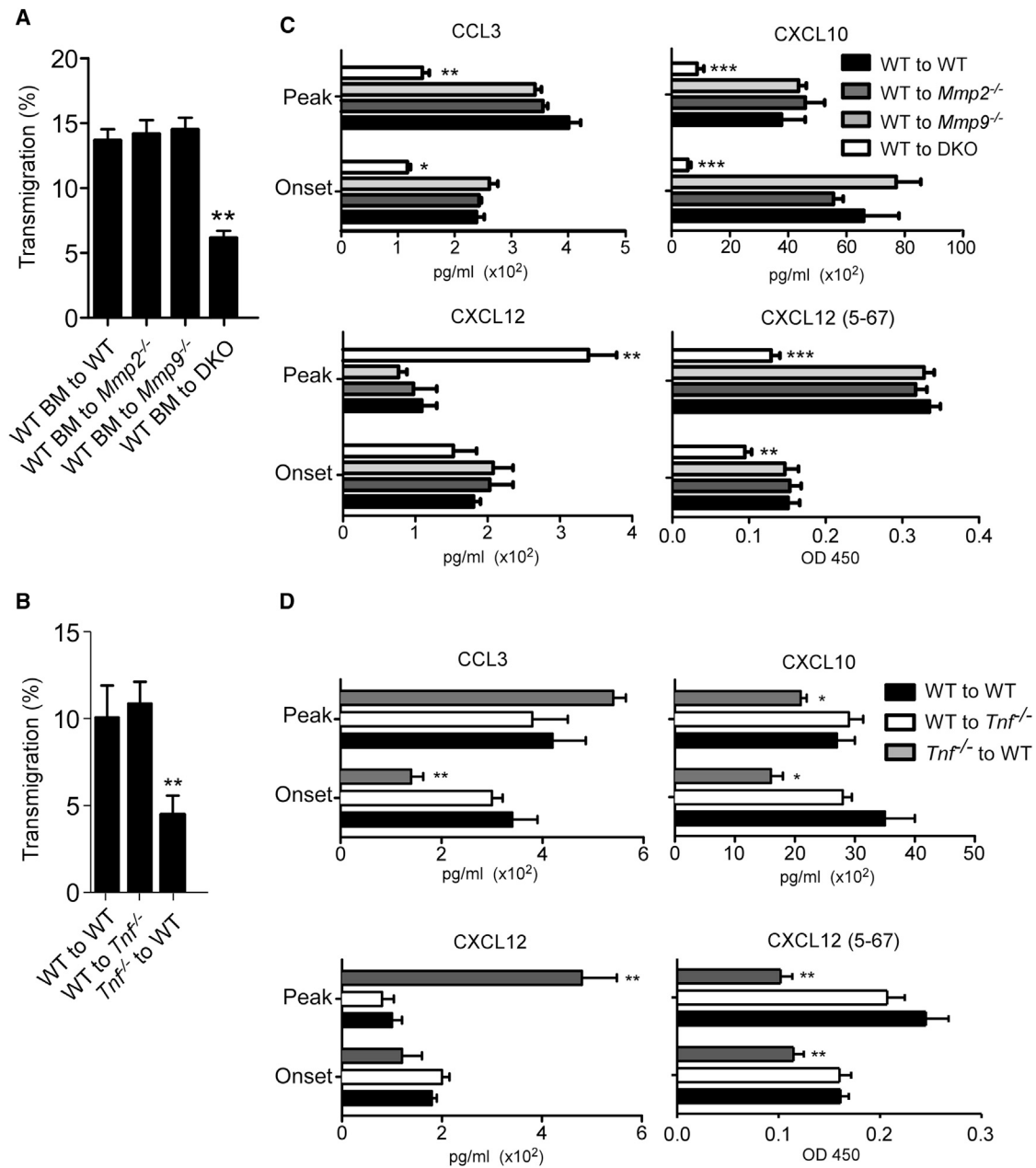
Figure 4. MMP-2/9 and Cytokines Are Required for Chemokine Secretion in the CNS

(A–D) Chemotactic potential of CNS extracts isolated at peak EAE (day 20) from (A) MMP-2/9 DKO chimeric mice and from (B) mice adoptively transferred with encephalitogenic WT or $Tnf^{-/-}$ T cells and (C and D) corresponding chemokine levels measured by ELISA in CNS extracts at EAE onset and peak. Data for CXCL12 are for full-length + cleaved chemokine and cleaved chemokine only (CXCL12 5-67). Data are means of four experiments with six mice/group ± SEM. *p < 0.05, **p < 0.01, ***p < 0.001. See also Figure S5.

potential of CNS extracts collected at peak EAE from MMP BM chimeric mice and from $Tnf^{-/-}$ adoptive transfer experiments. CNS extracts were added to the bottom chamber of a transwell system and primary CD4+ encephalitogenic T cells were placed in the top chamber. Transmigrated cells were counted at 6 hr. CNS extracts from WT or $Mmp2^{-/-}$ and $Mmp9^{-/-}$ chimeric mice had approximately the same chemotactic potential, which was signficantly reduced in CNS extracts from mice lacking a tis-

sue-resident source of MMP-2 and MMP-9 (Figure 4A) or lacking a T cell source of TNF-α (Figure 4B). To identify the missing chemotactic factor/s, the major chemokines implicated in EAE (CCL2, CCL3, CCL5, CCL20, CXCL10, and CXCL12) (Glabinski et al., 2005; Huang et al., 2000) were measured in CNS extracts at early and peak EAE. Significantly lower levels of all chemo-kines were measured in mice lacking tissue-resident sources of MMP-2 and MMP-9 or T cell-derived TNF-α, with the
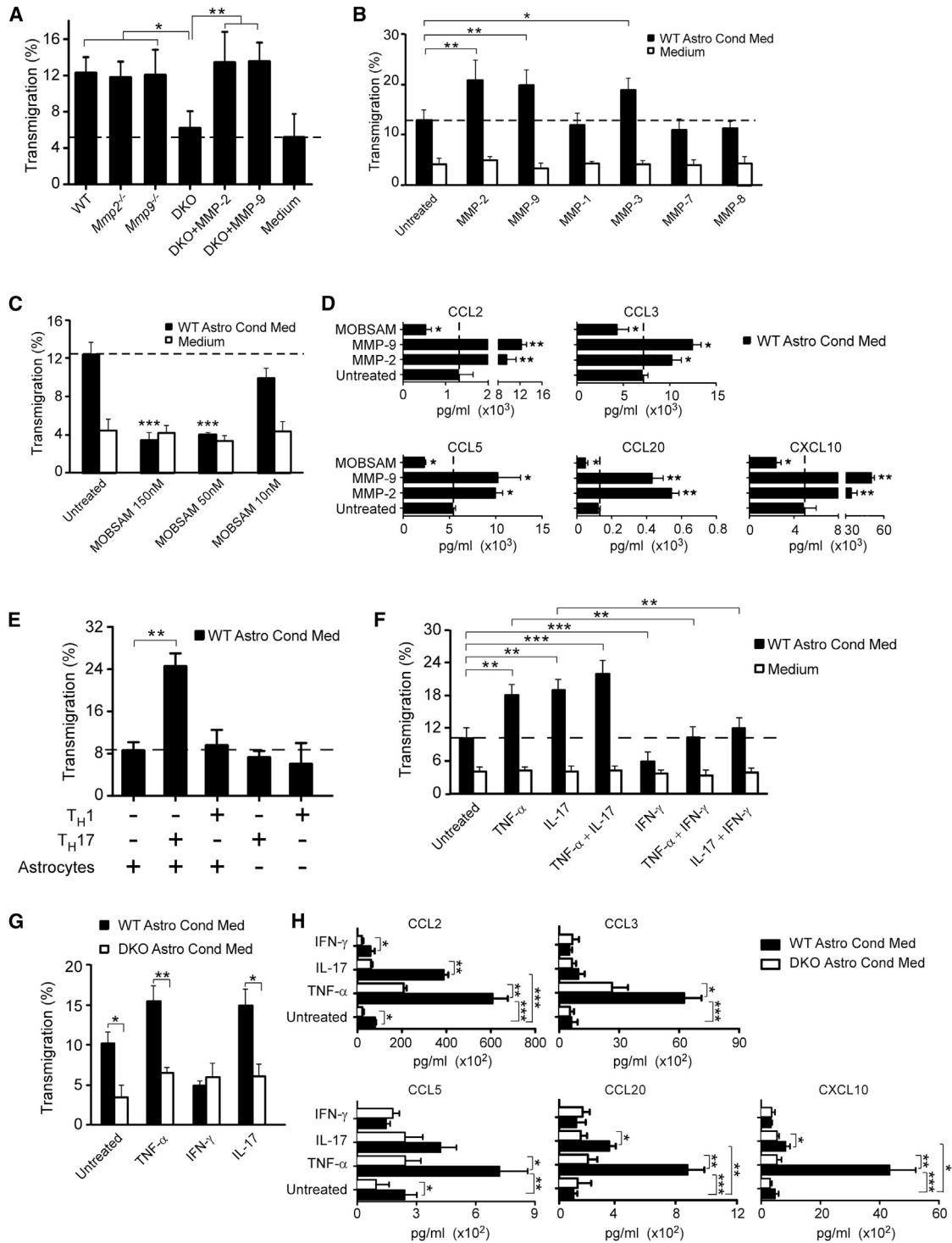
Figure 5. T Cell-Derived Cytokines Enhance Astrocyte Chemotactic Potential Only when MMP-2 or MMP-9 Is Present

(A) Transmigration of encephalitogenic T cells in response to conditioned media from irradiated WT, $Mmp2^{-/-}$, $Mmp9^{-/-}$, or DKO astrocytes in the presence or absence of activated MMP-2 or MMP-9.

(B–D) (B) Chemotactic potential of WT astrocyte-conditioned medium is enhanced by treatment with MMP-2 and MMP-9 or the progelatinase activator MMP-3, but not by MMPs-1, -7, or -8, and (C) reduced by inhibition of MMP activity by 50 or 150 nM MOBSAM; (D) corresponding chemokine levels in conditioned media of WT astrocytes treated with activated MMP-2 or MMP-9 or 50 nM MOBSAM.

(legend continued on next page)

exception of CXCL12, which was elevated at peak EAE in all situations (Figures 4C, 4D, S5A, and S5B). As MMP-2 and MMP-9 inactivate CXCL12 (Vergote et al., 2006), we also measured cleaved inactivated CXCL12, revealing significantly reduced levels in mice lacking MMP-2 and MMP-9 or T cell-derived TNF-α, suggesting higher levels of full-length CXCL12 (Figures 4C and 4D).

Astrocyte-Derived MMP-2 and MMP-9 Enhance T Cell Chemotaxis

As astrocytes express chemokines (Ambrosini et al., 2005; Glabinski et al., 1995; Kim et al., 2014) and, as shown here, MMP-2 and MMP-9, and they are strategically located at the parenchymal border, we utilized cultured astrocytes from WT and DKO mice to examine whether a relationship exists between MMPs and chemotactic potential. Conditioned media from WT-, *Mmp2*−/−-, *Mmp9*−/−-, or DKO-cultured astrocytes were used as chemoattractants in the lower chamber of a transwell system, and primary encephalitogenic T cells were placed in the upper chamber. Transmigrated cells were measured by flow cytometry after 6 hr. WT, *Mmp2*−/−, and *Mmp9*−/− astrocyte-conditioned media showed a basal chemotactic potential not present in DKO-conditioned medium (Figure 5A), which was enhanced by the addition of activated MMP-2, MMP-9, or MMP-3, but not other MMPs (Figure 5B). MMP-3 activates MMP-2 and MMP-9 (Ogata et al., 1992) and thereby probably increased the activated fraction of endogenous MMP-2 and MMP-9 present in the astrocyte-conditioned medium. Conversely, the basal chemotactic activity of WT astrocyte-conditioned medium was inhibited by MOBSAM, a chemical inhibitor that shows concentration-dependent inhibition of specific MMPs (Matsumura et al., 2005). Low doses of MOBSAM (10 nM) inhibit MMP-2 activation only, whereas 50 nM MOBSAM inhibits both MMP-2 and MMP-9 and >100 nM inhibits MMP-8, MMP-12, and MMP-13 (Matsumura et al., 2005). As no suppression of astrocyte chemotactic activity was observed at 10 nM MOBSAM, whereas 50 nM and 150 nM showed the same degree of inhibition (Figure 5C), this indicates that MMP-2 and MMP-9 are sufficient for regulation of the astrocyte-derived chemotactic activity. The data suggest that astrocytes could be a source of chemotactic factors for encephalitogenic T cells, the activity of which is enhanced by MMP-2 or MMP-9.

ELISA was used to investigate whether this chemotactic potential correlated with chemokine levels in the conditioned media. WT astrocyte-conditioned medium contained CCL2, CCL3, CCL5, CCL20, and CXCL10 (Figure 5D). CXCL12 was not detectable and is considered to be secreted by perivascular cells (McCandless et al., 2006). Treatment of WT astrocytes with activated MMP-2 or MMP-9 increased the levels of all detectable chemokines, while inhibition of MMP activation with 50 nM MOBSAM had a suppressive effect (Figure 5D), consistent with the transmigration data and suggesting endogenous MMP expression by astrocytes.

Pro- and Anti-Inflammatory Cytokines Modulate T Cell Chemotaxis in a MMP-Dependent Manner

Since TNF-α and IFN-γ affect MMP levels, we investigated the chemotactic potential of astrocyte-conditioned media in the presence and absence of TNF-α or IFN-γ, and correlated this with measurable chemokine levels. To mimic the in vivo situation, astrocytes were coincubated with primary T_H1 or T_H17 cells, and the chemotactic potential of the conditioned media was tested. CFSE-labeled CD4$^+$ T cells were added to the upper chamber of a transwell system to distinguish them from T cells coincubated with astrocytes, and transmigrated CFSE$^+$ cells were quantified by flow cytometry after 12 hr. The chemotactic activity of the astrocytes was significantly enhanced by coincubation with WT T_H17 cells, which secrete TNF-α and IL-17, while coculture with T_H1 cells, which secrete TNF-α and IFN-γ, had little effect. T_H17 or T_H1 cells alone had no effect (Figure 5E). Enhanced chemotaxis also was measured when WT astrocytes were stimulated with TNF-α or IL-17, with TNF-α plus IL-17 having mild additive effects (Figure 5F). By contrast, conditioned medium from IFN-γ-treated astrocytes inhibited both the basal chemotactic activity of astrocyte-conditioned medium and suppressed the enhanced chemotactic effects of TNF-α and IL-17 (Figure 5F). In the absence of astrocytes, cytokines alone had no effect on T cell transmigration (Figure 5F). When the same experiments were performed with DKO astrocyte-conditioned media, the basal chemotactic potential and the enhancing effects of TNF-α and IL-17 were suppressed (Figure 5G), and were rescued by the addition of activated MMP-2 or MMP-9 (Figure 5A).

Corresponding measurement of EAE-relevant chemokines in the cytokine-treated astrocyte-conditioned media revealed the absence of a strict correlation between chemokine levels and measured chemotaxis. While TNF-α and IL-17 both enhanced transmigration, TNF-α but not IL-17 increased chemokine levels, and IFN-γ, which suppressed transmigration, did not consistently reduce chemokine levels (Figures 5H and S6). These data support a role for TNF-α alone or in combination with IL-17 in inducing chemokine secretion by astrocytes, but also reinforces the pivotal role of MMP-2 and MMP-9 on the efficacy of astrocyte-derived chemotactic factors. Consistent with transmigration data, DKO astrocyte-conditioned medium contained significantly lower levels of all chemokines and a reduced response to TNF-α, IL-17, and IFN-γ (Figure 5H). Together with the strong upregulation of chemokine levels in response to MMP-2/9 treatment of astrocytes, in particular CXCL10 (Figure 5D), this suggests that MMP-2 and MMP-9 may promote chemokine release by astrocytes.

(E and F) (E) Chemotactic activity of WT astrocytes is enhanced by coincubation with T_H17 but not T_H1 cells and by (F) TNF-α or IL-17, while IFN-γ has suppressive effects. TNF-α plus IL-17 have additive effects and IFN-γ inhibits the enhanced chemotactic effects of TNF-α and IL-17.

(G) DKO astrocyte-conditioned medium has reduced chemotactic potential, which is not affected by proinflammatory chemokines.

(H) Chemokine levels measured by ELISA in conditioned media from WT or DKO astrocytes treated with proinflammatory cytokines. Experiments were performed three times using different astrocyte preparations, with triplicates/treatment in each experiment. Data are means ± SEM. *p < 0.05,**p < 0.01,***p < 0.001. See also Figure S6.
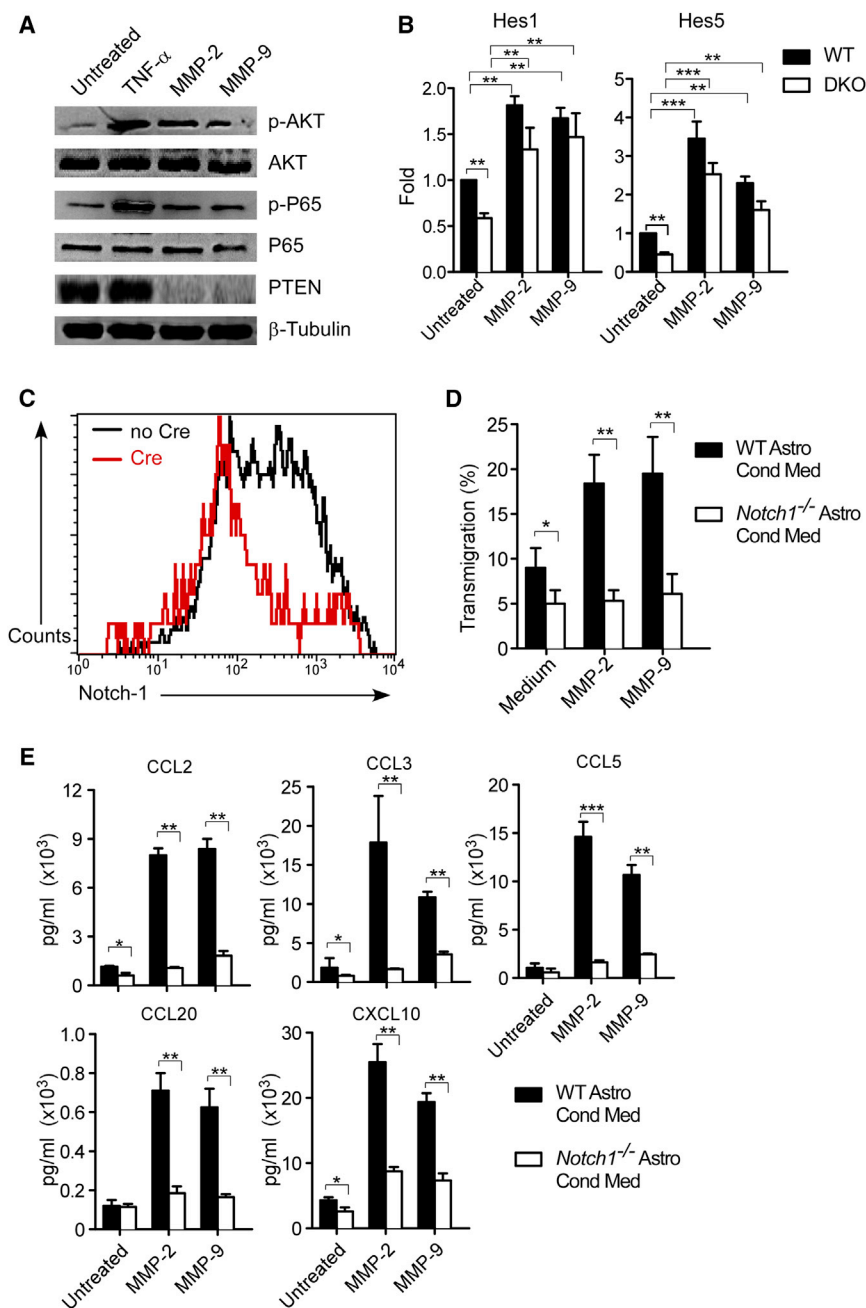
Figure 6. Signaling Pathway of MMP-2- and MMP-9-Induced Chemokine Secretion by Astrocytes

(A) Western blots for AKT/pAKT, p65/p-P65, and PTEN in cell extracts from untreated and TNF-α-, MMP-2-, and MMP-9-treated WT astrocytes. β-Tubulin is the loading control.

(B) Quantification of qPCR data for Notch-1-induced transcription factors, Hes1 and Hes5, in untreated and MMP-2- and MMP-9-treated WT and DKO astrocytes. Data are expressed as fold differences over WT levels and are means ± SEM of three to four experiments with triplicates/treatment.

(C) Flow cytometry shows loss of Notch-1 expression on Notch-loxP astrocytes after Cre-recombinase treatment.

(D and E) (D) Conditioned media from $Notch1^{-/-}$ astrocytes show reduced chemotactic potential compared to WT astrocytes, (E) significantly reduced chemokine levels, and absence of MMP-2- or MMP-9-induced upregulation of chemokines. Data are means ± SEM of three to four experiments with three to six replicates. *$p < 0.05$,**$p < 0.01$, ***$p < 0.001$. See also Figure S7.

To determine how MMPs could enhance NF-κB signaling, we turned to two known cell-surface MMP substrates on astrocytes: (1) dystroglycan, which anchors astrocyte endfeet to the parenchymal basement membrane (Agrawal et al., 2006); and (2) Notch-1, which is important for astrocyte development (Cau and Blader, 2009). Dystroglycan can signal via PI3K/p-AKT in skeletal muscle, but only when anchored to one of its ligands, laminin (Langenbach and Rando, 2002). As MMP-2 and MMP-9 cleave dystroglycan on astrocytes, disconnecting it from its ligands in the parenchymal basement membrane (Agrawal et al., 2006), it is unlikely to be associated with increased NF-κB signaling. By contrast, cleavage of Notch-1 by MMP-9 can lead to the inhibition of PTEN, thereby upregulating PI3K/p-AKT and NF-κB signaling (Garg et al., 2010). Western blots revealed inhibition of PTEN by MMP-2 or MMP-9 treatment of WT astrocytes (Figure 6A), and a corresponding upregulation of Notch-1-specific transcription factors, Hes1 and Hes5 (Figure 6B). DKO astrocytes showed reduced Hes1 and Hes5 expression, which was rescued by the addition of MMP-2 or MMP-9 (Figure 6B). $Notch-1^{-/-}$ astrocytes (Figure 6C) showed reduced basal chemotactic activity that was not rescued by MMP-2 or MMP-9 (Figure 6D), and showed no upregulation of chemokines in response to MMP-2 or MMP-9 treatment (Figure 6E). Control experiments with dystroglycan KO ($Dag^{-/-}$) astrocytes (Figure S7A) showed no difference

MMP-2 and MMP-9 Induce Chemokine Expression

We therefore investigated whether MMP-2 and MMP-9 of astrocytes impact on the major pathway associated with chemokine expression, namely PI3K/p-AKT/necrosis factor κB (NF-κB) (Quinones et al., 2008; Thompson and Van Eldik, 2009; van Loo et al., 2006). Western blots revealed that MMP-2- or MMP-9-treated astrocytes had increased levels of phosphorylated AKT and p-P65 (Figure 6A), suggesting increased NF-κB translocation to the nucleus. Similar effects were observed with TNF-α (Figure 6A), which is known to induce chemokine expression via NF-κB signaling (Quinones et al., 2008; Thompson and Van Eldik, 2009).
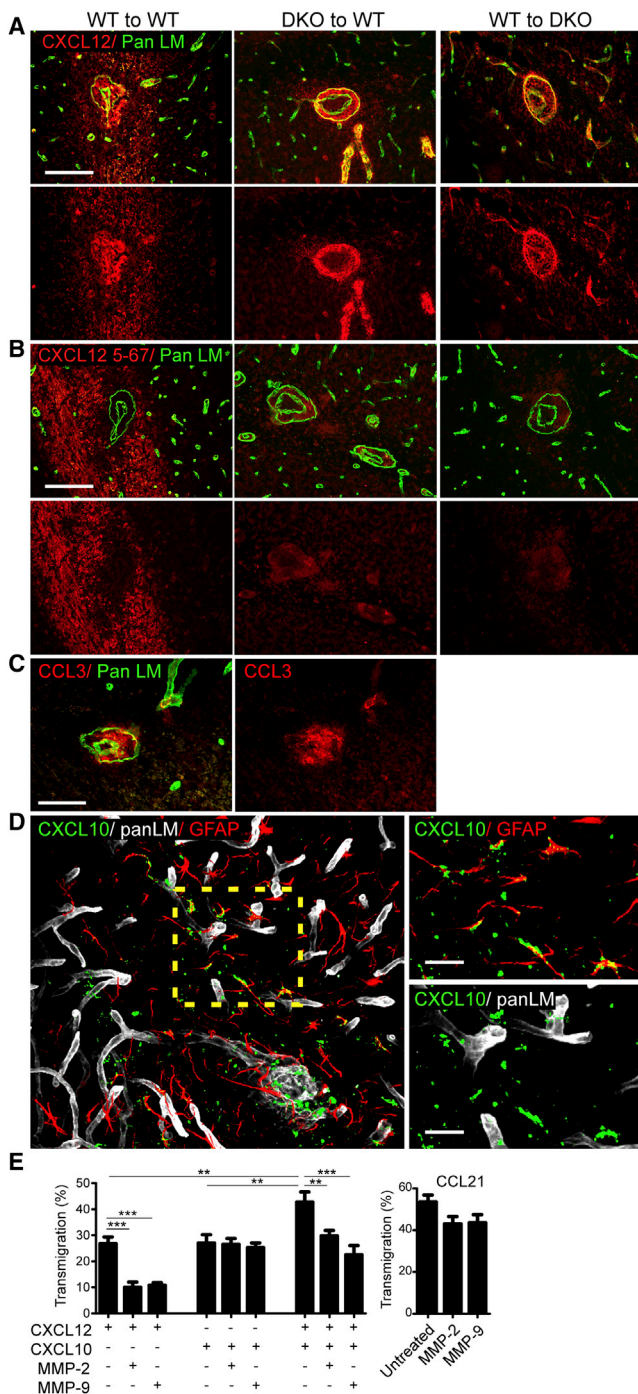
Figure 7. Differential Localization of Intact and MMP-Cleaved CXCL12, CCL3, and CXCL10 during EAE

(A) Brain sections from WT mice carrying WT (WT to WT) or DKO BM (DKO to WT) and DKO mice carrying WT BM mice (WT to DKO) were immunofluorescently stained at peak EAE for full-length and cleaved CXCL12 and pan laminin, revealing concentration within cuffs.

(B) Consecutive sections were stained for pan-laminin and cleaved CXCL12 only (CXCL12 5-67), revealing cleaved CXCL12 in the CNS parenchyma of WT to WT BM chimeras only.

(C and D) (C) Staining of WT brains at peak EAE for pan-laminin and CCL3 revealed expression only in cuffs, while (D) triple staining for pan-laminin,

compared to WT astrocytes in basal chemotactic potential, T cell transmigration in response to MMP-2 or MMP-9 (Figure S7B), or upregulation of chemokines (Figure S7C). Hence, MMP-2 and MMP-9 may stimulate Notch-1 signaling in astrocytes, leading to the inhibition of PTEN and subsequent induction of p-AKT/ NF-κB-signaling pathways and enhanced chemokine secretion.

MMP-2 and MMP-9 Also Modulate Chemokine Availability at the Parenchymal Border

MMP-2 and MMP-9 also can modulate chemokine activity or availability by selective cleavage (Van den Steen et al., 2000, 2003). While this is likely to occur in EAE, it is technically impossible to prove as it requires quantities of chemokines and their fragments for detection that cannot be extracted from the low numbers of small perivascular cuffs. We therefore analyzed the in vivo localization of key EAE chemokines in perivascular cuffs and at the parenchymal border using the antibodies available (CXCL12, CCL3, and CXCL10) in immunofluorescence confocal microscopy. CCL2, a further critical EAE chemokine that is inactivated by MMPs (McQuibban et al., 2002), was not investigated, as it has been extensively studied by others showing broad distribution in the cuff and CNS parenchyma (Paul et al., 2014). Since CXCL12 is inactivated by MMP-2 and MMP-9 (McQuibban et al., 2001), we employed an antibody that recognizes full-length and cleaved CXCL12, and another antibody that recognizes only cleaved, inactive CXCL12 (CXCL12 5-67) (Vergote et al., 2006). Triple staining for pan-laminin, CD45, and CXCL12 antibodies localized CXCL12 within cuffs and in the surrounding CNS parenchymal at onset and peak EAE (Figure 7A). Staining for cleaved CXCL12 demonstrated its localization in the CNS parenchyma only (Figure 7B), indicating that cleavage not only inactivates CXCL12, but also releases it from local retention, as reported by others (De La Luz Sierra et al., 2004). In mice lacking an immune-cell or tissue-resident source of MMPs, staining with the antibody to full-length + cleaved CXCL12 was restricted to the perivascular cuffs, with little or no signal for cleaved CXCL12 (Figure 7B).

Staining for CCL3 was restricted to the perivascular cuffs (Figure 7C), while CXCL10 occurred mainly in the CNS parenchymal surrounding cuffs and was detected only upon leukocyte penetration of the parenchymal border (Figure 7D). Double staining with GFAP revealed its localization close to astrocytes (Figure 7D), as previously reported (Carter et al., 2007). Staining for CCL3 and CXCL10 were not altered in mice lacking MMPs (not shown).

CXCL12 and CCL3 are inactivated by MMP-2 and MMP-9 (McQuibban et al., 2001; Vergote et al., 2006). CXCL10 is cleaved by MMP-9 (Van den Steen et al., 2003). However, the effect of cleavage on its chemotactic activity has not been reported. We therefore tested whether the chemotactic effect of

CXCL10, and GFAP showed CXCL10 in the CNS parenchyma close to astrocytes. Scale bars in (A–D) represent 40 μm.

(E) Transmigration of primary encephalitogenic T cells in response to CXCL10 or CXCL12 alone or together, in the presence and absence of MMP-2 or MMP-9. Transmigration in response to CCL21 ± MMP-2 or MMP-9 are controls. Data are means ± SEM of three experiments with triplicates/treatment. **p < 0.01, ***p < 0.001.

CXCL10 for encephalitogenic T cells is altered by MMP-2/9 treatment using a transwell system. To mimic the in vivo situation, CXCL12 and CXCL10 were added alone or together, in the presence or absence of MMP-2 or MMP-9. Comparisons were made with CCL21, as an example of a chemokine that is not cleaved by MMPs. MMP-2 or MMP-9 treatment of CXCL12 significantly reduced its chemotactic potential but had no effect on CXCL10, while CXCL12 plus CXCL10 had additive effects that were reduced to levels measured with CXCL10 alone in the presence of MMP-2 or MMP-9 (Figure 7E).

Hence, MMP-2/9 derived from infiltrating cells or CNS-resident cells can inactivate CXCL12 and CCL3, releasing inactivated CXCL12 into the CNS parenchyma and permitting infiltrating T cells to respond to other chemokines in the CNS parenchyma, such as CXCL10, which are not affected by the MMPs.

DISCUSSION

Leukocyte penetration of the parenchymal border is a rate-limiting step in the induction of EAE symptoms (Agrawal et al., 2006; Toft-Hansen et al., 2006). We showed here that both immune-cell and tissue-resident sources of MMP-2 and MMP-9 are required for this step and act specifically at the parenchymal border to promote leukocyte migration out of the perivascular cuff. We showed that the balance of leukocyte-derived inflammatory cytokines, TNF-α versus IFN-γ, regulate mainly MMP-9 secretion and activation by astrocytes at the parenchymal border, which can impact on levels and/or activity of chemokines that attract the encephalitogenic T cells into the CNS to induce EAE symptoms. TNF-α and IL-17 promote MMP-9, and to a lesser extent MMP-2, secretion and activation, while IFN-γ acts as a negative regulator of their secretion and activation, as reported in other systems (Di Girolamo et al., 2006; Ho et al., 2008).

In the absence of a CNS-resident source of MMP-2 and MMP-9, immune cell migration to the CNS and into the perivascular cuff was not altered. However, cuffs were larger and penetration of the parenchymal border and onset of disease symptoms were significantly delayed, which correlated with significantly lower levels of most of the EAE-relevant chemokines in the CNS, with the notable exception of CXCL12, and reduced clinical symptoms. This is consistent with previous reports that CNS-specific chemokine mRNA expression never precedes histological signs of EAE (Huang et al., 2000), and that initial leukocyte infiltration into the CNS is a prerequisite for intrathecal expression of chemokines (Glabinski et al., 1995). The initial recruitment of T cells to the CNS is likely to be controlled by CXCL12, which has been shown by others to hold immune cells in the perivascular cuff (McCandless et al., 2006), and which we show here is present in its intact form only within the perivascular cuff.

We propose that once the right balance of Th1/Th17 cells in the perivascular cuff is reached, and thereby the ratio of TNF-α and IL-17 versus IFN-γ is elevated, secretion of mainly activated MMP-9 by astrocytes at the parenchymal border is enhanced. The critical role of proinflammatory cytokines released from infiltrating T cells in this step was demonstrated by transfer of encephalitogenic $Tnf^{-/-}$ T cells to WT recipients, also resulting in enlarged perivascular cuffs and delayed onset of EAE symp-

toms, reduced CNS chemokine levels, and, most importantly, suppressed gelatinase activity, as observed in mice lacking a resident MMP-2/9 source. Apart from the absence of TNF-α, we show that $Tnf^{-/-}$ T cells have significantly elevated IFN-γ levels, but otherwise normal levels of other cytokines, reinforcing that it is not just the absence of TNF-α but rather the balance of different cytokines that modulates MMP secretion and activity at the inflammatory front.

We demonstrated a pivotal role for MMP-2 and MMP-9 activity, rather than chemokine levels per se, in promoting T cell migration. Conditioned medium from WT astrocytes constitutively expressed pro-MMP-2 and activated MMP-2 and low levels of pro-MMP-9, which correlated with a basal chemotactic potential that was absent in DKO astrocyte-conditioned medium or when MMP activation was chemically inhibited. This constitutive expression of MMP-2 in the brain (Rosenberg, 2002) probably accounts for leukocyte recruitment during immune surveillance and at EAE induction. However, under inflammatory conditions we showed that TNF-α strongly upregulates not only chemokine expression by astrocytes (Ambrosini et al., 2005), but also astrocyte MMP-9, and to lesser extent MMP-2, expression and activation, which might enhance chemotactic potential, but only when the astrocytes are capable of secreting active MMP-2 or MMP-9. This is consistent with published data that upregulation of chemokines by intracerebral injection of TNF-α is not sufficient to cause accumulation of leukocytes in the CNS (Glabinski et al., 2003).

By contrast, the effects of IL-17 and IFN-γ on chemokine secretion varied and did not correlate with their enhancing and suppressive effects, respectively, on T cell chemotaxis. Rather, gel zymography, ELISA, and qPCR suggested that IFN-γ also can suppress secretion and activation of MMP-9, as reported previously (Di Girolamo et al., 2006), while IL-17 synergizes with TNF-α to induce both chemokine secretion and MMP expression/activation, and importantly compensates for TNF-α in its absence, as observed in the $Tnf^{-/-}$ mice. These data are consistent with the previously reported moderate effects of IFN-γ on chemokine secretion by astrocytes and with EAE data from $Ifng^{-/-}$ mice, which have exacerbated disease symptoms but reduced expression of several key EAE chemokines, including CXCL10, CCL5, and CCL2 (Carter et al., 2007; Tran et al., 2000), and only moderate upregulation of CCL3 and CCL1 (Tran et al., 2000). The fact that ablation of astrocyte-derived MMP-2 and MMP-9 activity, either chemically (MOBSAM) or via the use of DKO astrocytes, also significantly reduced the chemotactic capacity of astrocytes, and that this could not be reversed by cytokine treatment but only by MMP-2 or MMP-9 substitution, suggests a key role for the MMPs in chemotaxis. Apart from astrocytes, other sources of MMPs, such as microglial or perivascular cells (McCandless et al., 2006; Meiron et al., 2008), cannot be excluded and may contribute in vivo. In addition, immune cells also can contribute to MMP-2 and MMP-9 at the parenchymal border, as suggested by the EAE experiments performed with DKO mice carrying WT BM.

MMP-2 and MMP-9 can promote early leukocyte migration across the parenchymal border in several ways, including selective cleavage to modulate chemokine activity and/or availability (Van den Steen et al., 2000, 2003) or promotion of chemokine

secretion or release by astrocytes. Our data suggest that both occur in EAE. It is impossible in our model to define precisely which chemokines are affected in which way by the MMPs, due to the limitations of even the most sophisticated mass spectrometry technologies for quantitative analysis of chemokines and their fragments in the small inflammatory foci, and due to the limited availibility of reagents for in vivo chemokine detection. However, this is not the critical point, but rather that MMP-2 or MMP-9 is essential at the inflammatory front and can modulate EAE-relevant chemokines by cleavage and/or induction of their expression, which impacts on whether or not leukocytes can breach the inflammatory front. We demonstrated that one way in which MMP-2 and MMP-9 may induce chemokine expression by astrocytes is via activation of the AKT/NF-κB-signaling pathway (Quinones et al., 2008; Thompson and Van Eldik, 2009) in a Notch-1-dependent manner. Notch-1 is expressed by astrocytes (Cau and Blader, 2009) and is cleaved by MMP-9 (Garg et al., 2010), and possibly also MMP-2, thereby resulting in the inhibition of PTEN and activation of the Akt/NF-κB axis (Garg et al., 2010; van Loo et al., 2006). However, other pathways are not excluded and require investigation.

A role for MMP-2 and MMP-9 in modulating the activity or availability of chemokines acting on infiltrating leukocytes is supported by the observation that CXCL12 levels were significantly elevated in mice lacking either an immune-cell or tissue-resident source of MMP-2 and MMP-9, while the corresponding levels of the cleaved/inactive form were reduced. Further, although TNF-α is a potent inducer of chemokine secretion by WT astrocytes, TNF-α stimulation of DKO astrocytes could not promote T cell transmigration, and the pro-migration effects of TNF-α/IL-17 and the suppressive effects of IFN-γ were ablated by the inhibition of MMP-2 and MMP-9 and did not strictly correlate with chemokine levels. We showed here that CXCL12 is present in perivascular cuffs of postcapillary venules in the active/uncleaved form, thereby retaining leukocytes in the cuff (McCandless et al., 2006) and probably accounting for the enlarged cuffs observed in the MMP chimeric mice. However, CXCL12 that is expressed or diffuses toward the cuff border and into the CNS parenchyma is inactivated due to the presence of activated MMP-2/9, permitting leukocytes to respond to other chemokines, such as CXCL10, which we showed are localized outside of the cuff and strongly upregulated by MMP-2/9, but not otherwise modulated by MMP-2/9.

Other chemokines such as CCL3 and CCL2 that are abundant in the inflamed CNS are also cleaved by MMP-2/9, resulting in fragments that bind antagonistically to their receptors (McQuibban et al., 2000, 2002). Given the broad spectrum of chemokines that are expressed simultaneously in the CNS during EAE, and the varied effects of MMP-2/9 on the different chemokines, it is likely that the sum of these effects determines whether or not the disease-inducing T cells can breach the inflammatory front to induce EAE symptoms. This highlights the strength of a functional readout, as used here, to evaluate chemotactic potential.

In conclusion, during inflammation TNF-α and IL-1 versus IFN-γ and IL-17 balance leukocyte migration through induction and/or inhibition of chemokines. We demonstrated that their chemotactic effects are mediated, at least in part, by MMP-9 and MMP-2, and localized these effects to the inflammatory front. Our data illustrate that the cytokine-MMP-chemokine axis defines a network that governs whether or not leukocytes can breach the inflammatory front to transmigrate the parenchymal border and induce disease symptoms. Rather than a single cytokine, the ratio of stimulatory and regulatory cytokines orchestrates leukocyte movement across the parenchymal barrier, features that are relevant to other inflammatory conditions. Although previous studies have implicated MMP-2/9 in EAE and human MS, our data demonstrate that it is not MMP activity per se but rather its in vivo localization that is crucial. The activation of MMP-2/9 precisely at the parenchymal border by cytokines, and, thereby, activation of chemotactic signals at this border, means that, once the leukocytes have transmigrated across the parenchymal border and entered into the CNS parenchyma, the cytokine levels decrease and the chemotactic signal is switched off. This provides initially a self-perpetuating system that then becomes self-limiting, simply by the migration of the leukocytes across the parenchymal border into the CNS parenchyma, a mechanism that would not require high MMP levels but rather depends on the strategic localization of activated MMPs.

EXPERIMENTAL PROCEDURES

Animals

Mice employed were C57BL/6, Tnf⁻/⁻ (Körner et al., 1997), Mmp2⁻/⁻ (Itoh et al., 1997), Mmp9⁻/⁻ (Dubois et al., 1999), Notch-1-loxP (Radtke et al., 1999), and dystroglycan-loxP mice (Moore et al., 2002). Mmp2⁻/⁻ and Mmp9⁻/⁻ mice were bred to generate double KO (DKO) and heterozygous littermate controls. Experiments were conducted according to German Animal Welfare guidelines.

Antibodies

Antibodies used in immunofluorescence, flow cytometry, and cell sorting were from BD Pharmingen or eBioscience unless otherwise stated: pan-laminin (455), CD45 (30G.12), CD45.2 (104), CD45.1 (A20), CD11b/MAC-1 (M1/70), CD4 (H129.19), Foxp3 (NRRF-30), IL-17 (TC11-18H10.1), IFN-γ (XMG1.2), IL-6 (MP5-20F3), IL-10 (JES5-16E3), IL-4 (11B11), IL-2 (JES6-5H4), TNF-α (MP6-XT22) and CD16/CD32 (2.4G2), myelin basic protein (PA1050, Boster Biological Technology) and glial-fibrillar-acidic protein (G-A-5, Sigma-Aldrich), CXCL12 (AHP794, AbD Serotec), CXCL10 (AF-466, R&D Systems), CCL3 (ab25128, Abcam), and dystroglycan (Vimsa) (Agrawal et al., 2006).

Immunohistochemistry

Immunofluorescence stainings were performed as described previously (Agrawal et al., 2006). To measure cuff sizes, brains and spinal cords were oriented in the same position and sectioned entirely from dorsal to ventral. Bound antibodies were visualized using Alexa 488- or Cy3-conjugated goat anti-rat, Cy3- or Cy5-conjugated anti-rabbit secondary antibodies (Jackson ImmunoResearch Laboratories and Molecular Probes), and FITC-anti-CD45 (104, eBioscience). Sections were examined using a Zeiss AxioImager equipped with epifluorescent optics or a Zeiss LSM 700 confocal microscope, and documented using a Hamamatsu ORCA ER camera.

Stainings for CXCL10 required fixation of whole brains in 4% paraformaldehyde (PFA) for 90 min at 4°C, embedding in 4% agarose, and sectioning into 200-μm sections. Sections were blocked in 4% normal goat serum plus 3% BSA in 0.5% Triton X-100. Primary and secondary antibody incubations were performed overnight at 4°C. Stainings for CCL3 and the cleaved form of CXCL12 functioned only on 5–10-μm cryosections.

MMPs and Inhibitors

Recombinant MMPs were from R&D Systems. p-Aminophenylmercuric acetate (APMA; Sigma-Aldrich) was used to activate MMP-1, MMP-7, and MMP-8. MMP-3 was employed to activate MMP-2 and MMP-9. MOBSAM, an N-sulphonylamino acid derivative, provided by Shionogi and Company, is

a dose-dependent inhibitor of MMPs (Matsumura et al., 2005). qPCR for MMP-2 and MMP-9 mRNAs was performed using primers listed in the Supplemental Experimental Procedures.

Active and Passive EAE

EAE was induced using 35–55 peptide of myelin oligodendrocyte glycoprotein (MOG$_{35-55}$). Passive transfer of encephalitogenic T cells was as described previously (Wu et al., 2009). EAE onset was defined by weight loss and appearance of a limp tail. Peak EAE was between days 20 and 25 after immunization or T cell transfer.

BM Chimeric Mice

WT or DKO BM cells were transferred i.v. (5×10^6 per mouse) to lethally irradiated (11 Gy) congenic recipients (WT, $Mmp2^{-/-}$, $Mmp9^{-/-}$, or DKO mice). Polymorphic lineage determinants (CD45.1/CD45.2) were used for tracking donor- versus host-derived immune cells.

In Vitro T Cell Differentiation

MOG$_{35-55}$-specific CD4$^+$ T cells were cultured in RPMI medium, 10% FCS, and 20 μg/ml MOG$_{35-55}$ for 2 days, and then in the presence of IL-2 (10 ng ml^{-1}) for another 2 days. IL-12 (10 ng ml^{-1}) and anti-IL-4 (10 μg ml^{-1}) were added for T$_H$1 differentiation, or IL-23 (10 ng ml^{-1}), IL-1β (10 ng ml^{-1}), anti-IFN-γ (10 μg ml^{-1}), and anti-IL-4 (10 μg ml^{-1}) for T$_H$17 differentiation, and cultured for another 5 days.

MRI

MRI measurements to determine brain volumes were performed before and after EAE on a 3T Philips Achieva System (Philips Healthcare) equipped with a 4-cm solenoidal radio frequency coil with heater to maintain body temperature. Mice were anaesthetized by continuous inhalation of 1.5% isoflurane. No gating or triggering during the measurements was used. A 3D gradient echo dataset was acquired in 9:50-min scan time using the following parameters: isotropic resolution, 200 μm, reconstructed to $90 \times 90 \times 200$ μm^3; field of view (FOV), $20 \times 16 \times 8$ mm^3; echo time/repetition time (TE/TR), 5.1/18 ms; excitation pulse angle, 35°; averages, 10. The brain was segmented semi-manually using the lasso-tool in the software package amira (Visage Imaging), and the volume was calculated.

Stereology

Following MRI, brains and spinal cords were excised, weighed, and sectioned entirely (ventral to dorsal; approximately 1,000 sections of 5–6 μm/brain); 1 in every 50 sections was stained for CD45 and pan-laminin, and cuff numbers and areas were measured using Volocity 5.5 (Improvision). At least four individual mice per group (i.e., WT, $Tnf^{-/-}$, DKO mice transferred with WT T cells) were analyzed.

In Situ Hybridization

Frozen sections of EAE brains were fixed in 4% PFA and in situ hybridization was performed as described previously (Frieser et al., 1997), with the exception that riboprobes were labeled with digoxigenin (DIG)-UTP and detected by sheep anti-digoxygenin alkaline phosphatase, followed by alkaline phosphatase reaction using nitrotetrazolium blue chloride and 5-bromo-4-chloro-3-indolyl. After in situ hybridization, sections were stained with GFAP-Cy3 (Sigma-Aldrich) and DAPI, and imaged using a Zeiss AxioImager. The 385-bp mouse MMP-9 cDNA was generated by PCR using the following primers: 5′CATTCGCGTGGATAAGGA3′ and 5′ACAAGAAAGGACGGTGGG 3′.

Cytometric Bead Array

CD4$^+$ T cells (2×10^5) were cultured in RPMI medium with MOG$_{35-55}$ for 2 days as described above, and cytokine levels in conditioned media were measured using Cytomix kit (Bender MedSystems). All chemokines, except CCL20 and CXCL12, in tissue extracts and conditioned media were measured using Chemomix kit (Bender MedSystems).

ELISA

Full-length CXCL12 was measured using the mouse CXCL12/SDF-1 alpha Quantikine ELISA kit (R&D); for cleaved CXCL12, the primary antibody was re-placed by anti-CXCL12 5-67 (Vergote et al., 2006) and data were expressed as OD$_{450}$ values. CCL20 levels were measured using mouse CCL20 Quantikine ELISA kit (R&D). MMP-2 and MMP-9 activities were measured using the QuickZyme kit (QuickZyme Biosciences).

Flow Cytometry

Mice were perfused with PBS before spleens, LNs, and brains were harvested. Spleens and brains were treated with 2 μg ml^{-1} collagenase D (Roche Diagnostics) and 1 μg ml^{-1} DNase I (Roche Diagnostics), and cells were isolated by cell straining (70 μm spleens/100 μm brains). Brain homogenates were separated into neuronal and leukocyte populations by discontinuous density gradient centrifugation using isotonic Percoll (Amersham). The intracellular staining kit (eBioscience) was employed to permeabilize and fix cells, and flow cytometry was performed using a FACS Calibur (Becton Dickinson). Delta-like protein/Fc chimera (R&D) and TRITC-labeled goat anti-mouse IgG Fc (Jackson ImmunoResearch) were employed in flow cytometry for detection of astrocyte expression of Notch-1.

Gelatin Zymography

Gelatin gel and in situ zymography coupled with immunofluorescence staining were performed as described previously (Agrawal et al., 2006), with the exception that centrifugation concentrated (Amicon) and gelatin-Sepharose prepurified astrocyte condition media were employed in gel zymography. Conditioned media from confluent 48-hr cultures were pooled, concentrated, and purified before use in gel zymography.

Astrocyte Culture

Primary astrocyte cultures were prepared from brains of newborn WT, $Mmp2^{-/-}$, $Mmp9^{-/-}$, and DKO mice as described previously (Agrawal et al., 2006). Serum-free F12 medium from astrocyte cultures was collected at 24–48 hr for use in in vitro transmigration assays, gel zymography, and chemokine secretion measurements. In some cases, astrocytes were cultured overnight in serum-free F12 plus TNF-α (50 ng ml^{-1}); IFN-γ (300 unit ml^{-1}); IL-17 (500 ng ml^{-1}); recombinant activated MMP-2 (100 ng ml^{-1}) and/or MMP-9 (20 ng ml^{-1}); or 10, 50, or 150 nM MOBSAM.

Astrocytes were isolated from newborn Notch-1-*loxP* and dystroglycan-*loxP* mice. Cells were treated with 2 μM recombinant cre-recombinase protein (HTNC) for 20 hr, washed, and cultured in F12 medium for 1 week before testing by flow cytometry using anti-β-dystroglycan antibody or Delta-like protein/Fc chimera plus TRITC-labeled goat anti-mouse IgG Fc.

Transmigration Assays

Transmigration studies were performed with T cells isolated from spleens and LNs at day 14 or 17 after EAE induction using anti-CD4-coated MACS beads. Cells (0.7×10^6) in 100 μl serum-free DMEM were placed in the upper chamber of a transwell filter (Costar, 5 μm), and transmigration was induced by adding 600 μl serum-free F12 astrocyte-conditioned medium to the lower chamber, 0.1–1 μg ml^{-1} recombinant chemokines (CXCL12, CXCL10, CCL21) (Promokine) alone, or chemokines plus activated MMP-2 or MMP-9. Experiments were conducted at 37°C for 6 hr, after which the number of cells that had transmigrated into the lower chamber were counted and expressed as a percentage of the total cells added.

Notch-1 Signaling

qPCR was used to determine mRNA expression of Hes-1 and Hes-5 using the primers listed in the Supplemental Experimental Procedures. For Notch-1-signaling experiments, astrocytes were untreated or treated for 24 hr with 50 ng ml^{-1} TNF-α and recombinant activated MMP-2 or MMP-9. Cells were lysed and analyzed by western blotting using the following antibodies: PTEN (D4.3, Cell Signaling Technology), p65 (C22B4, Cell Signaling Technology), Phospho-NF-κB p65 (93H1, Cell Signaling Technology), Phospho-IkB-α (14D4, Cell Signaling Technology), Phospho-AKT (Biosource), total Akt (C67E7, Cell Signaling Technology), and β-Tubulin (Epitomics).

Statistical Analyses

Statistical analyses were performed using GraphPad Prism. All values are expressed as means ± SEM. Data were tested for normality (Kolmogorov-Smirnov

test in GraphPad Prism). If there was no normal distribution, then we used the non-parametric Mann-Whitney or Kruskal-Wallis test, otherwise we employed the two-sided Student's t test or ANOVA.

SUPPLEMENTAL INFORMATION

Supplemental Information includes Supplemental Experimental Procedures and seven figures and can be found with this article online at http://dx.doi.org/10.1016/j.celrep.2015.01.037.

AUTHOR CONTRIBUTIONS

ACKNOWLEDGMENTS

REFERENCES

Agrawal, S., Anderson, P., Durbeej, M., van Rooijen, N., Ivars, F., Opdenakker, G., and Sorokin, L.M. (2006). Dystroglycan is selectively cleaved at the parenchymal basement membrane at sites of leukocyte extravasation in experimental autoimmune encephalomyelitis. J. Exp. Med. 203, 1007–1019.

Ambrosini, E., Remoli, M.E., Giacomini, E., Rosicarelli, B., Serafini, B., Lande, R., Aloisi, F., and Coccia, E.M. (2005). Astrocytes produce dendritic cell-attracting chemokines in vitro and in multiple sclerosis lesions. J. Neuropathol. Exp. Neurol. 64, 706–715.

Carter, S.L., Müller, M., Manders, P.M., and Campbell, I.L. (2007). Induction of the genes for Cxcl9 and Cxcl10 is dependent on IFN-gamma but shows differential cellular expression in experimental autoimmune encephalomyelitis and by astrocytes and microglia in vitro. Glia 55, 1728–1739.

Cau, E., and Blader, P. (2009). Notch activity in the nervous system: to switch or not switch? Neural Dev. 4, 36–47.

Corry, D.B., Rishi, K., Kanellis, J., Kiss, A., Song Lz, L.Z., Xu, J., Feng, L., Werb, Z., and Kheradmand, F. (2002). Decreased allergic lung inflammatory cell egression and increased susceptibility to asphyxiation in MMP2-deficiency. Nat. Immunol. 3, 347–353.

De La Luz Sierra, M., Yang, F., Narazaki, M., Salvucci, O., Davis, D., Yarchoan, R., Zhang, H.H., Fales, H., and Tosato, G. (2004). Differential processing of stromal-derived factor-1alpha and stromal-derived factor-1beta explains functional diversity. Blood 103, 2452–2459.

Di Girolamo, N., Indoh, I., Jackson, N., Wakefield, D., McNeil, H.P., Yan, W., Geczy, C., Arm, J.P., and Tedla, N. (2006). Human mast cell-derived gelatinase B (matrix metalloproteinase-9) is regulated by inflammatory cytokines: role in cell migration. J. Immunol. 177, 2638–2650.

Dubois, B., Masure, S., Hurtenbach, U., Paemen, L., Heremans, H., van den Oord, J., Sciot, R., Meinhardt, T., Hämmerling, G., Opdenakker, G., and Arnold, B. (1999). Resistance of young gelatinase B-deficient mice to experimental autoimmune encephalomyelitis and necrotizing tail lesions. J. Clin. Invest. 104, 1507–1515.

Engelhardt, B. (2006). Molecular mechanisms involved in T cell migration across the blood-brain barrier. J. Neural Transm. 113, 477–485.

Frieser, M., Nöckel, H., Pausch, F., Röder, C., Hahn, A., Deutzmann, R., and Sorokin, L.M. (1997). Cloning of the mouse laminin alpha 4 cDNA. Expression in a subset of endothelium. Eur. J. Biochem. 246, 727–735.

Garg, P., Sarma, D., Jeppsson, S., Patel, N.R., Gewirtz, A.T., Merlin, D., and Sitaraman, S.V. (2010). Matrix metalloproteinase-9 functions as a tumor suppressor in colitis-associated cancer. Cancer Res. 70, 792–801.

Glabinski, A.R., Tani, M., Tuohy, V.K., Tuthill, R.J., and Ransohoff, R.M. (1995). Central nervous system chemokine mRNA accumulation follows initial leukocyte entry at the onset of acute murine experimental autoimmune encephalomyelitis. Brain Behav. Immun. 9, 315–330.

Glabinski, A.R., Bielecki, B., Kolodziejski, P., Han, Y., Selmaj, K., and Ransohoff, R.M. (2003). TNF-alpha microinjection upregulates chemokines and chemokine receptors in the central nervous system without inducing leukocyte infiltration. J. Interferon Cytokine Res. 23, 457–466.

Glabinski, A., Jalosinski, M., and Ransohoff, R.M. (2005). Chemokines and chemokine receptors in inflammation of the CNS. Expert Rev. Clin. Immunol. 1, 293–301.

Hartupee, J., Liu, C., Novotny, M., Li, X., and Hamilton, T. (2007). IL-17 enhances chemokine gene expression through mRNA stabilization. J. Immunol. 179, 4135–4141.

Ho, H.H., Antoniv, T.T., Ji, J.D., and Ivashkiv, L.B. (2008). Lipopolysaccharide-induced expression of matrix metalloproteinases in human monocytes is suppressed by IFN-gamma via superinduction of ATF-3 and suppression of AP-1. J. Immunol. 181, 5089–5097.

Huang, D., Han, Y., Rani, M.R., Glabinski, A., Trebst, C., Sørensen, T., Tani, M., Wang, J., Chien, P., O'Bryan, S., et al. (2000). Chemokines and chemokine receptors in inflammation of the nervous system: manifold roles and exquisite regulation. Immunol. Rev. 177, 52–67.

Itoh, T., Ikeda, T., Gomi, H., Nakao, S., Suzuki, T., and Itohara, S. (1997). Unaltered secretion of beta-amyloid precursor protein in gelatinase A (matrix metalloproteinase 2)-deficient mice. J. Biol. Chem. 272, 22389–22392.

Kim, R.Y., Hoffman, A.S., Itoh, N., Ao, Y., Spence, R., Sofroniew, M.V., and Voskuhl, R.R. (2014). Astrocyte CCL2 sustains immune cell infiltration in chronic experimental autoimmune encephalomyelitis. J. Neuroimmunol. 274, 53–61.

Körner, H., Riminton, D.S., Strickland, D.H., Lemckert, F.A., Pollard, J.D., and Sedgwick, J.D. (1997). Critical points of tumor necrosis factor action in central nervous system autoimmune inflammation defined by gene targeting. J. Exp. Med. 186, 1585–1590.

Langenbach, K.J., and Rando, T.A. (2002). Inhibition of dystroglycan binding to laminin disrupts the PI3K/AKT pathway and survival signaling in muscle cells. Muscle Nerve 26, 644–653.

Matsumura, S., Iwanaga, S., Mochizuki, S., Okamoto, H., Ogawa, S., and Okada, Y. (2005). Targeted deletion or pharmacological inhibition of MMP-2 prevents cardiac rupture after myocardial infarction in mice. J. Clin. Invest. 115, 599–609.

McCandless, E.E., Wang, Q., Woerner, B.M., Harper, J.M., and Klein, R.S. (2006). CXCL12 limits inflammation by localizing mononuclear infiltrates to the perivascular space during experimental autoimmune encephalomyelitis. J. Immunol. 177, 8053–8064.

McQuibban, G.A., Gong, J.H., Tam, E.M., McCulloch, C.A., Clark-Lewis, I., and Overall, C.M. (2000). Inflammation dampened by gelatinase A cleavage of monocyte chemoattractant protein-3. Science 289, 1202–1206.

McQuibban, G.A., Butler, G.S., Gong, J.H., Bendall, L., Power, C., Clark-Lewis, I., and Overall, C.M. (2001). Matrix metalloproteinase activity inactivates the CXC chemokine stromal cell-derived factor-1. J. Biol. Chem. 276, 43503–43508.

McQuibban, G.A., Gong, J.H., Wong, J.P., Wallace, J.L., Clark-Lewis, I., and Overall, C.M. (2002). Matrix metalloproteinase processing of monocyte

chemoattractant proteins generates CC chemokine receptor antagonists with anti-inflammatory properties in vivo. Blood *100*, 1160–1167.

Meiron, M., Zohar, Y., Anunu, R., Wildbaum, G., and Karin, N. (2008). CXCL12 (SDF-1alpha) suppresses ongoing experimental autoimmune encephalomy-elitis by selecting antigen-specific regulatory T cells. J. Exp. Med. *205*, 2643–2655.

Moore, S.A., Saito, F., Chen, J., Michele, D.E., Henry, M.D., Messing, A., Cohn, R.D., Ross-Barta, S.E., Westra, S., Williamson, R.A., et al. (2002). Deletion of brain dystroglycan recapitulates aspects of congenital muscular dystrophy. Nature *418*, 422–425.

Murphy, C.A., Hoek, R.M., Wiekowski, M.T., Lira, S.A., and Sedgwick, J.D. (2002). Interactions between hemopoietically derived TNF and central nervous system-resident glial chemokines underlie initiation of autoimmune inflamma-tion in the brain. J. Immunol. *169*, 7054–7062.

Ogata, Y., Enghild, J.J., and Nagase, H. (1992). Matrix metalloproteinase 3 (stromelysin) activates the precursor for the human matrix metalloproteinase 9. J. Biol. Chem. *267*, 3581–3584.

Paul, D., Ge, S., Lemire, Y., Jellison, E.R., Serwanski, D.R., Ruddle, N.H., and Pachter, J.S. (2014). Cell-selective knockout and 3D confocal image analysis reveals separate roles for astrocyte-and endothelial-derived CCL2 in neuroin-flammation. J. Neuroinflammation *11*, 10.

Quinones, M.P., Kalkonde, Y., Estrada, C.A., Jimenez, F., Ramirez, R., Mahi-mainathan, L., Mummidi, S., Choudhury, G.G., Martinez, H., Adams, L., et al. (2008). Role of astrocytes and chemokine systems in acute TNFalpha induced demyelinating syndrome: CCR2-dependent signals promote astrocyte activa-tion and survival via NF-kappaB and Akt. Mol. Cell. Neurosci. *37*, 96–109.

Radtke, F., Wilson, A., Stark, G., Bauer, M., van Meerwijk, J., MacDonald, H.R., and Aguet, M. (1999). Deficient T cell fate specification in mice with an induced inactivation of Notch1. Immunity *10*, 547–558.

Ransohoff, R.M. (2009). Chemokines and chemokine receptors: standing at the crossroads of immunobiology and neurobiology. Immunity *31*, 711–721.

Rosenberg, G.A. (2002). Matrix metalloproteinases in neuroinflammation. Glia *39*, 279–291.

Sixt, M., Engelhardt, B., Pausch, F., Hallmann, R., Wendler, O., and Sorokin, L.M. (2001). Endothelial cell laminin isoforms, laminins 8 and 10, play decisive roles in T cell recruitment across the blood-brain barrier in experimental auto-immune encephalomyelitis. J. Cell Biol. *153*, 933–946.

Thompson, W.L., and Van Eldik, L.J. (2009). Inflammatory cytokines stimulate the chemokines CCL2/MCP-1 and CCL7/MCP-3 through NFkB and MAPK dependent pathways in rat astrocytes [corrected]. Brain Res. *1287*, 47–57.

Toft-Hansen, H., Buist, R., Sun, X.J., Schellenberg, A., Peeling, J., and Owens, T. (2006). Metalloproteinases control brain inflammation induced by pertussis toxin in mice overexpressing the chemokine CCL2 in the central nervous sys-tem. J. Immunol. *177*, 7242–7249.

Tran, E.H., Prince, E.N., and Owens, T. (2000). IFN-gamma shapes immune in-vasion of the central nervous system via regulation of chemokines. J. Immunol. *164*, 2759–2768.

Van den Steen, P.E., Proost, P., Wuyts, A., Van Damme, J., and Opdenakker, G. (2000). Neutrophil gelatinase B potentiates interleukin-8 tenfold by amino-terminal processing, whereas it degrades CTAP-III, PF-4, and GRO-alpha and leaves RANTES and MCP-2 intact. Blood *96*, 2673–2681.

Van den Steen, P.E., Husson, S.J., Proost, P., Van Damme, J., and Opdenak-ker, G. (2003). Carboxyterminal cleavage of the chemokines MIG and IP-10 by gelatinase B and neutrophil collagenase. Biochem. Biophys. Res. Commun. *310*, 889–896.

van Loo, G., De Lorenzi, R., Schmidt, H., Huth, M., Mildner, A., Schmidt-Supprian, M., Lassmann, H., Prinz, M.R., and Pasparakis, M. (2006). Inhibition of transcription factor NF-kappaB in the central nervous system ameliorates autoimmune encephalomyelitis in mice. Nat. Immunol. *7*, 954–961.

Vergote, D., Butler, G.S., Ooms, M., Cox, J.H., Silva, C., Hollenberg, M.D., Jha-mandas, J.H., Overall, C.M., and Power, C. (2006). Proteolytic processing of SDF-1alpha reveals a change in receptor specificity mediating HIV-associated neurodegeneration. Proc. Natl. Acad. Sci. USA *103*, 19182–19187.

Weaver, C.T., Hatton, R.D., Mangan, P.R., and Harrington, L.E. (2007). IL-17 family cytokines and the expanding diversity of effector T cell lineages. Annu. Rev. Immunol. *25*, 821–852.

Wu, C., Ivars, F., Anderson, P., Hallmann, R., Vestweber, D., Nilsson, P., Ro-benek, H., Tryggvason, K., Song, J., Korpos, E., et al. (2009). Endothelial base-ment membrane laminin alpha5 selectively inhibits T lymphocyte extravasation into the brain. Nat. Med. *15*, 519–527.